Analytica Chimica Acta 1189 (2022) 339222

Contents lists available at ScienceDirect

Analytica Chimica Acta

journal homepage: www.elsevier.com/locate/aca

Graphene oxide nanosheet-mediated fluorescent RPA "turn-on" biosensor for rapid RNAi transgenic plant detection

Kai Li [a], Zhan Lei [b], Chen Zhang [b], Longjiao Zhu [c], Kunlun Huang [a, **], Ying Shang [b], Wentao Xu [a, c, *]

[a] Key Laboratory of Safety Assessment of Genetically Modified Organism (Food Safety) (MOA), Beijing Laboratory for Food Quality and Safety, College of Food Science and Nutrition Engineering, China Agricultural University, Beijing, 100191, China
[b] Faculty of Agriculture and Food, Kunming University of Science and Technology, Kunming, Yunnan, 650500, China
[c] Key Laboratory of Precision Nutrition and Food Quality, Department of Nutrition and Health (Institute of Nutrition and Health) , China Agricultural University, Beijing 100083, China

HIGHLIGHTS

- Graphene oxide (GO) nanosheets enhanced the thermostatic fluorescent biosensor for rapid RNAi plant detection.
- The aggregation of the GO-absorbing ingredients of the RPA reaction increased amplification efficiency.
- RPA triggered the conversion of the fluorescence-labeled primer inducing the recovery of the GO quenched signal.
- This biosensor achieved the on-site detection of RNAi soybeans at a concentration as low as 1.5 ng genome DNA in 20 min.
- GO participated in the RPA amplification process, forming unique "blanket"-like structures.

GRAPHICAL ABSTRACT

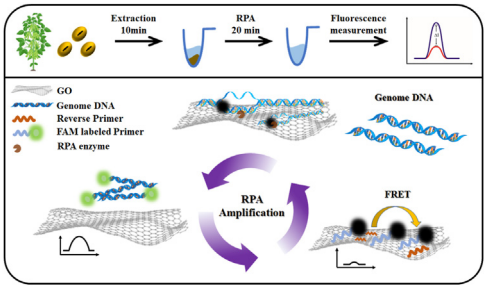

ARTICLE INFO

Article history:
Received 2 August 2021
Received in revised form
11 October 2021
Accepted 26 October 2021
Available online 29 October 2021

Keywords:
Recombinase polymerase amplification
Graphene oxide nanosheets
Nucleic acid

ABSTRACT

In this paper preliminarily verified that graphene oxide (GO) nanomaterials enhanced the recombinase polymerase amplification (RPA). GO nanosheets improved the efficiency of RPA amplification by absorbing ingredients to induce local aggregation. The recombinase initially aggregated with the primers to form nucleoprotein filaments, absorbed on the GO nanosheets, changing the structure. Therefore, an isothermal fluorescence biosensor was developed based on GO nanosheets enhanced the RPA to detect RNA interference (RNAi) transgenic plants. FAM-labeled primers were absorbed and quenched by the GO nanosheets. After amplification, the primers were extended into double-stranded DNA, detaching from the GO surface to recover the fluorescent signal. The biosensor displayed high sensitivity and selectivity and showed an excellent relationship ranging from 1.5 to 100 ng of genome DNA, with a detection limit

* Corresponding author. Key Laboratory of Safety Assessment of Genetically Modified Organism (Food Safety) (MOA), Beijing Laboratory for Food Quality and Safety, College of Food Science and Nutrition Engineering, China Agricultural University, Beijing, 100191, China.
** Corresponding author.
E-mail addresses: hkl009@163.com (K. Huang), xuwentao@cau.edu.cn (W. Xu).

https://doi.org/10.1016/j.aca.2021.339222

Rapid detection
Biosensor

(LOD) of 1.5 ng. Consequently, the biosensor provides an enhanced isothermal method for detecting genetically modified (GM) products and exhibits significant potential for molecular detection.

1. Introduction

As functional elements, nanomaterials have been widely used in chemistry [1], medicine [2], biology [3,4] and environmental science [5,6]. The performance enhancement of DNA amplification in molecular diagnosis using nanomaterials has attracted increasing attention. Gold nanoparticles [7–9], single-walled carbon nanotubes [10], silicon nanowires [11,12], TiO_2 nanoparticles [13], carbon nano-powder [14], and graphene nanosheets [15] promote the efficiency of the PCR reaction via superior thermal conductivity and the potential ability to act as catalysts in reactions. However, minimal studies are available involving the enhancement of isothermal amplification using nanoscale particles or nanoflakes. In addition, the enhancement theory based on the PCR results is insufficient, requiring more evidence regarding morphology and the interaction between nanomaterials and reaction reagents. Moreover, nanomaterials are typically multi-functional, but the reported detection methods for nucleic acid *in vitro* lack rapidity, visualization, and portability.

PCR, as the "gold standard" method in nucleic acid analysis has been widely used in detecting plants [16], cells [17], bacteria [18], and viruses [19]. However, PCR is time costing, complicated and needs temperature cyclers and professionals [20], restricting its application in POC test. Isothermal amplification strategized were proposed to address these issues. Specifically, enzymatic isothermal amplification reactions have been considered to detect DNA targets. Isothermal nucleic acid amplification is an alternative for PCR and is ideally suited to point-of-care (POC) testing. The properties of these isothermal methods increase practical adaptability and applicability. However, verification of these amplification techniques mostly using nucleic acid dyes and ssDNA probes. The dye strategies lack specificity and increase the background signal. Furthermore, probes with multiple labels are not suitable for POC detection due to the high cost. As a new type of nanomaterial with excellent electronic, mechanical, optical, and thermal properties, graphene has received extensive attention and is rapidly applied in various fields. Graphene oxide (GO) is an essential derivative of graphene with a honeycomb lattice structure [21]. This unique structure and the abundant functional groups on the GO surface include excellent properties, such as extensive surface area [22], electron transfer capability [23], biocompatibility [24,25]. GO displays a strong capability to adsorb small molecules [26,27] to the surface through π-π stacking [28,29]. Due to the unique structure of GO, the fluorescence of dye molecules can be quenched via fluorescence resonance energy transfer (FRET) [30], displaying excellent quenching efficiency [31,32]. Furthermore, the extraordinary quenching efficiency of GO can increase sensitivity while decreasing the background signal of the fluorescence [33]. Therefore, GO nanomaterials provide a new approach for isothermal detection during POC testing.

The regulation of new biotechnology based transgenic plants is important for the development of genetically modified technology and the safety of consumers. Different from traditional genetically modified (GM) technique, RNA interference (RNAi) provides a gene silence at the transcriptional level, which also poses a new challenge for conventional detection methods. In this paper, GO nanosheets are examined to enhance the stability and amplification efficiency of the RPA reaction. Consequently, a GO nanosheet-mediated fluorescent RPA biosensor (GORB) for rapidly detecting DNA targets is described. In addition, the fluorescent GORB is used for RNAi transgenic plant detection. An excellent relationship is evident in a range of 1.5–100 ng, with a limit of detection (LOD) of 1.5 ng. The biosensor shows significant potential for molecular detection.

2. Material and methods

2.1. Reagents and materials

The RNAi transgenic plant events (E2D8037-3 soybean) were stored in the laboratory. GM maize (MON810 and Bt11) and soybeans (MON89788 and MON87705) were purchased from the American Oil Chemists Society (AOCS) and the Institute of Reference Materials (IRMM). GM rice (TT51 and Kefeng 6) and non-GM seed samples were previously stored in the laboratory. The chloroform, DNA phenol extraction reagent, Plant Genomic DNA Kit, Trans 2 K Marker, and 6xDNA loading buffer were purchased from TransGen Biotech Company (Beijing, China). Agarose, 1x TAE buffer, EDTA, acetic acid and absolute ethyl alcohol were purchased from Merck Chemical Company (Darmstadt, Germany). Double distilled water (ddwater) was used throughout the experiments. GO was purchased from XFNANO Biotech Company (Nanjing, China). The RPA amplification kit was purchased from TwistDx.

Table 2
GORB reaction system.

Reagent name	Added amount (μL)
Labeled F (10 μM)	1.5
Primer R (10 μM)	1.5
Primer-Free Rehydration buffer	29.5
Template	2
ddH_2O	8
GO	5
Mg^{2+}	2.5
Total volume	50

Table 1
Sequences of the DNA probes used in this work.

Primer	Primer sequence (5′ to 3′)	Product sizes (bp)
RPA-F	ACTCCCAATGACAACATTTTTTCGTAATAACATTT	428
RPA-R	TTGAACGATAGCCTTTCCTTTATCGCAATGATGGC	
Labeled -F	FAM-ACTCCCAATGACAACATTTTTTCGTAATAACATTT	

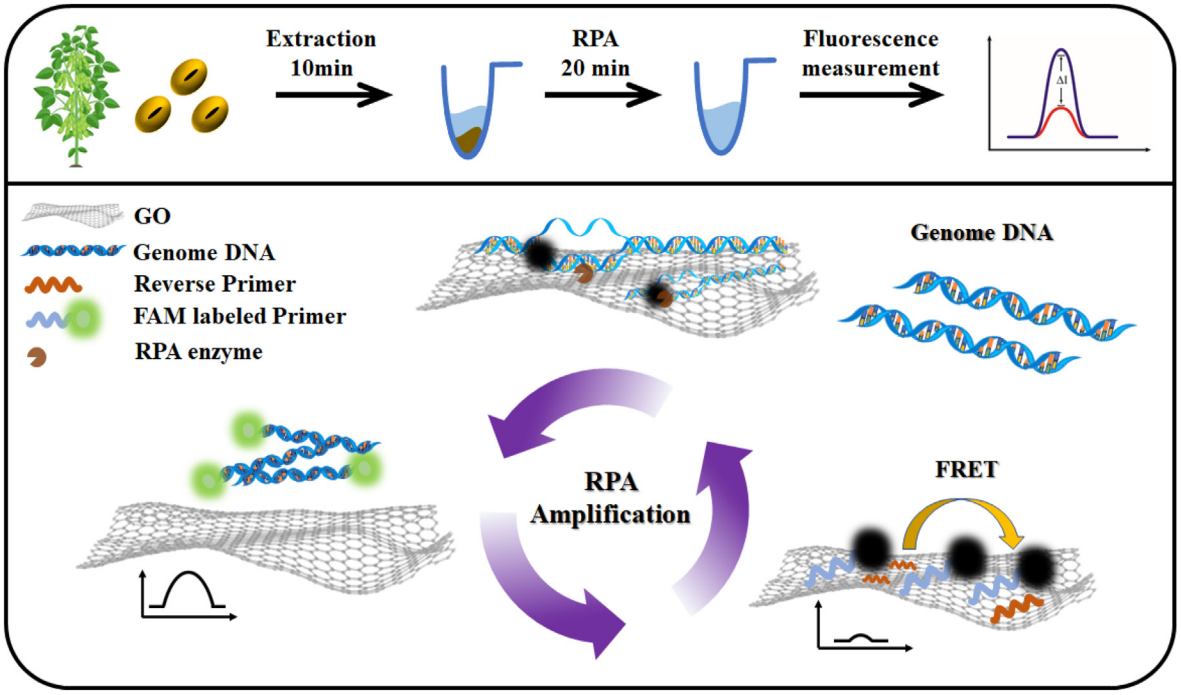

Scheme 1. Schematic illustration of GM detection based on the RPA and fluorescence quenching of GO.

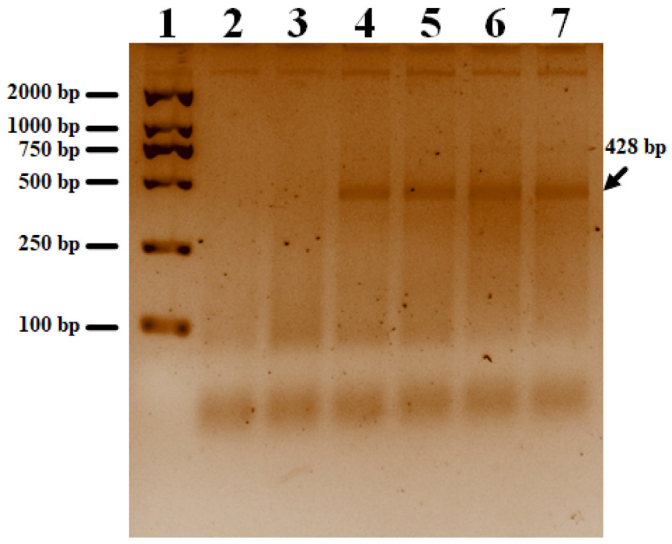

Fig. 1. Agarose gel electrophoresis image of the RPA products. Lane 1: The DNA marker (100–2000 bp). Lane 2–3: The negative soybean sample DNA. Lane 3–4: The RPA product without GO. Lane 6–7: The RPA product with GO (FAM-labeled forward primer, 10 μM; GO, 140 μg/mL).

2.2. Extraction and purification of DNA

The RNAi transgenic samples were extracted using a TIANcombi DNA lyse&Det PCR Kit (TransGen Biotech, Beijing, China) with some modifications. The seed samples were pulverized using a pulverizer. This process was performed with care to avoid cross-contamination between the samples. A 20 mg sample was placed in a 2.0 mL centrifugal tube containing 400 μL Buffer B1. After mixing thoroughly, 400 μL Buffer B2 was added and incubated in room temperature for several minutes. Then, DNA sample was centrifuge at 12000 rpm (~13400×*g*) for 2 min. After centrifugation, carefully move the 400 μL of the supernatant into another new tube. The DNA quality was analyzed using the NanoDrop one ultra-micro-UV Spectrophotometer (NanoDrop Technologies Inc., Wilmington, DE, USA) and electrophoresis on 2% agarose gel. The DNA solution was stored at 4 °C and used as DNA templates during subsequent analyses.

2.3. Design of event-specific RPA primers

The RPA primer design was performed on the left boundary flanking sequence of the exogenous insertion fragment. A total of upstream and downstream primer was designed during this screening. The corresponding screening was performed, followed by cross-number screening, to determine the optimal primer. The transgenic soybean primer sequence was about 30–38 bases in length. The oligonucleotide primers and fluorescent dye-labeled probes were designed using Primer 5 software and synthesized by Shanghai Sangon Co. Ltd. (Shanghai, China).

2.4. Electron microscopy analysis

The dispersed sample was dripped onto a copper sheet. After drying, the copper sheet containing the sample was attached to the conductive tape on the sample stand. Scanning electron microscopy (SEM) imaging and spectrum analysis were performed using an SEM system (JEOL, USA).

2.5. Optimization of the experimental conditions

To test the quenching effect of GO, various GO concentrations (0–160 μg/mL) were incubated with FAM labeled probes in ddwater at room temperature while subjected to gentle shaking for 10 min. The GO and probe mixtures were examined using a fluorescence spectrometer to determine whether the fluorescence was reduced. The optimal GO concentration was selected according to the fluorescence intensity. Then, the GO and the probes were

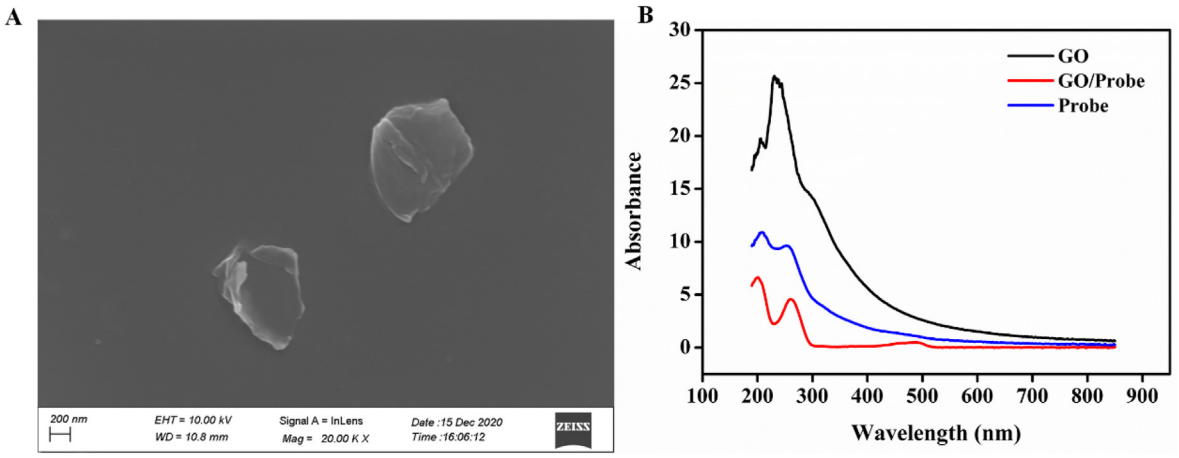

Fig. 2. The characterization of the GO nanosheet. A, SEM images of the GO nanosheets. B, The UV spectrum of the GO nanosheets.

incubated with transgenic soybeans using the RPA reaction for 5−30 min to identify the optimal interaction time between GO and the target.

2.6. Gel electrophoresis analysis

Gel electrophoresis analysis was performed on 2% (w/w) agarose gel stained with gel stain, after which gel imaging was performed using an SHST Capture Gel SH-510 (Hangzhou Shenhua Technology Co., Ltd., China).

2.7. Fluorescence measurement

Fluorescence measurements were carried out using an RF-6000 fluorescence spectrometer (Shimadzu, Japanese). The parameters were listed below. The excitation wavelength was set at 492 nm, while the emission starting wavelength was 510 nm−600 nm. The excitation and emission slit widths were set at 1.0 nm with a 6000 nm/min scan speed. The excitation and emission bandwidth were set to 5 nm. First, the cuvette was cleaned with ddwater, and 50 μL of ddwater was drawn for blank determination. Then, the samples were subjected to spectral measurements, which were repeated three times to determine the stability of the peak shape (see Table 1).

2.8. GORB for practical sample detection

The DNA extraction and purification of the RNAi transgenic soybean were performed according to step 2.2. Then, the genome DNA of target sample was added in GORB system which was listed in Table 2. The reaction mixture was 47.5 μL with rehydration buffer (29.5 μL), GOs (120 μg/mL, 5 μL), FAM-labeled forward primer (10 μM, 1.5 μL), reverse primer (10 μM, 1.5 μL) and genome DNA (2 μL). GO nanosheet was mixed with primer and incubated for 10 min before adding into the tube. The reaction mix was then added to the freeze-dried tube, which was flicked until the freeze-dried powder fully dissolved. To initiate the reaction, 2.5 μL of 280 mM magnesium acetate (MgAc) was added. Then tubes were immediately incubated for 20 min at 39 °C in a thermal cycler. Finally, the fluorescence of the RPA products was measured using a fluorescence spectrometer.

3. Results and discussion

3.1. Principle

This study designed a novel approach for GM detection by combining RPA with the fluorescence quenching of GO nanosheets, as shown in Scheme 1. Probes with fluorochrome for GM amplification were designed and synthesized. Due to the nature of GO single-chain adsorption, incubating the probes with GO allowed them to be absorbed on the surface of the GO nanosheets, revealing the quenched fluorescence signal. After GM incubation, the strand displacement exchange reaction occurred under the action of the single-stranded DNA binding protein, melting the template DNA. The probes and guide strand were combined to form new double-stranded DNA, while the passenger strand was combined with the single-stranded DNA binding protein to prevent further replacement, which was adsorbed by GO. Furthermore, under the action of strand displacement polymerase, the newly formed double-stranded DNA was used as an amplification template, causing an exponential increase in the amplified products. Due to the weak binding ability of GO to double-stranded DNA, the amplified products abandoned the GO surface to generate a fluorescent signal.

3.2. RPA amplification of RNAi transgenic plants

Standard RPA primers were designed to amplify the left border flanking sequence of the exogenous insert gene. A primer pair was enhanced after screening (Figure S2), while its specificity and sensitivity were examined (Figure S3 and S4). The length of the amplification product was 428 bp. A FAM-labeled forward primer was used to examine the RPA amplification ability with and without GO. Fig. 1 shows that labeled FAM and GO did not influence the RPA reaction.

3.3. Characterization of GO

All the characterization results of GOs used in this study were shown in Figure S1, including FTIR, XRD, XPS and TEM. The XRF results and properties of GOs were shown in Table S2 and Tables S3 respectively. The diameter of GOs was 500 nm to 5 μm and the thickness was 0.8−1.2 nm. The ratio of C:O was 2. The SEM image of the GO nanosheet is illustrated in Fig. 2A. The specific surface area of the GO nanosheets is extensive, allowing for the adsorption of more single-stranded DNA. The UV spectrum of the GO nanosheet,

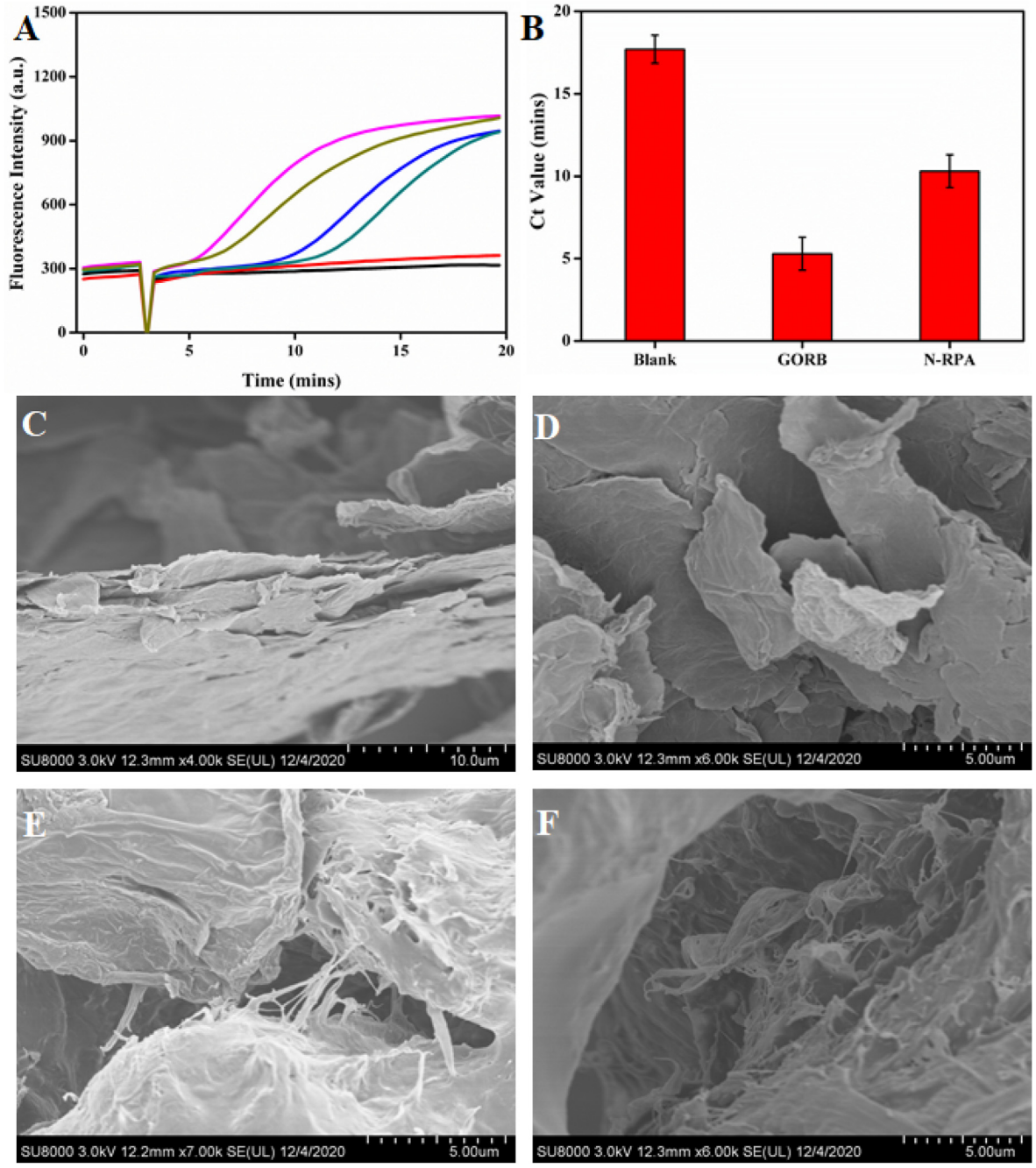

Fig. 3. The GO-enhanced RPA reaction. A, Fluorescent spectra of the GORB and N-RPA reaction over time. The fluorescence measurement was performed using a Twista tube scanning device (TwistDX, Cambridge, UK). The reaction was conducted at 39 °C for 30 min and measured every 20 s. The fluorescence spectra of GORB (pink and brown), N-RPA (blue and green), and Blank (red and black) were measured. B, The Ct value of GORB, N-RPA, and Blank. C and D, The SEM images of the standard RPA results. E and F, The SEM images of the GO-enhanced RPA results. (For interpretation of the references to color in this figure legend, the reader is referred to the Web version of this article.)

FAM-labeled primer, and a combination of the two is shown in Fig. 2B. The absorption peak of the GO nanosheet and primer was centered at 235 nm and 260 nm, respectively.

3.4. GO improved the performance of RPA

To examine the promotional effect of the GO nanosheets, the fluorescent method and SEM were selected to verify the amplification efficiency and morphological changes of the surface, respectively. The fluorescence-labeled forward primer combined with GO was used for the RPA reaction. For comparison, a fluorescence probe based on standard RPA and a blank control was applied using a Twista tube scanning device (TwistDX, Cambridge, UK). The real-time fluorescence results are shown in Fig. 3A. The threshold time value of these six samples is shown in Fig. 3B. The threshold of GORB occurred about 5 min after the reaction, which was five times faster than the standard RPA reaction (10 min). The blank samples showed no amplification curve. The time threshold comparison between GORB and N-RPA indicated that the GO nanosheet promoted the efficiency of RPA. In addition, the fluorescent RPA results obtained via a TwistAmp Exo kit (TwistDX, Cambridge, UK) showed a high signal at the beginning, which

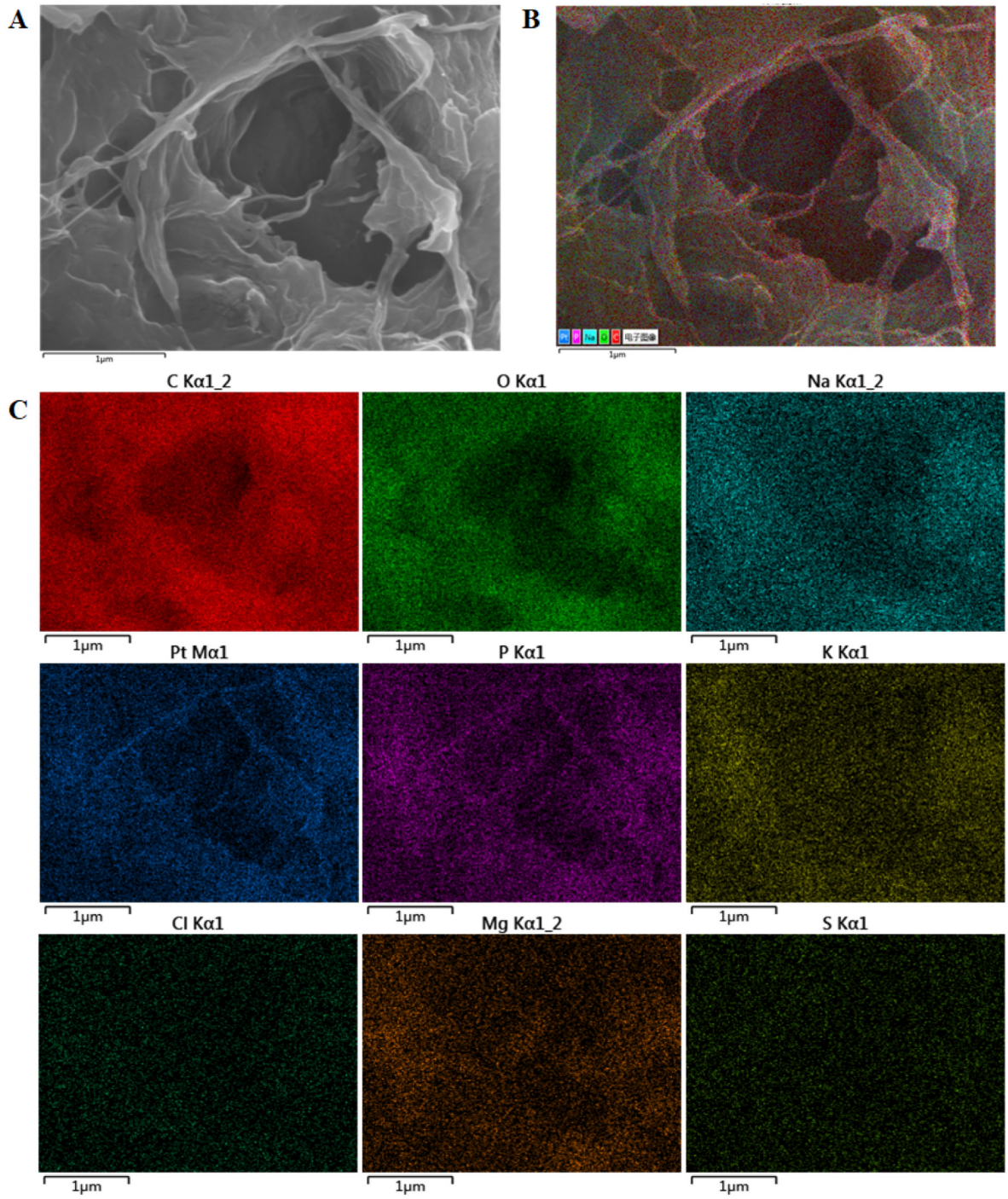

Fig. 4. The energy spectrum analysis of GORB. A, The SEM image of the GORB reaction. B, The element distribution in the microscopic areas of the GORB products. The position of the color represents the distribution of the element. The color intensity represents the content of different elements. C, Element analysis results, including C, O, Na, Pt, P, K, Cl, and Mg. (For interpretation of the references to color in this figure legend, the reader is referred to the Web version of this article.)

exceeded the reading range of the machine in some cases (Figure S5). The amplification curve exhibited a high background signal or one that was out of range. However, GORB displayed a low signal level initially while exhibiting a better amplification curve after the reaction (Figure S6). The ability to absorb and quench FAM-labeled ssDNA allowed the GO nanosheets to reduce the background signal before initiating the RPA reaction.

The nanomaterials absorbed the small molecules surrounding them, increasing the local concentration. This process caused the nanomaterials to aggregate, causing morphological changes. Furthermore, to examine how the GO nanosheets enhanced RPA, SEM was used to observe the morphological changes of GO in the presence and absence of the RPA reaction. The results are shown in Fig. 4. The surface and edges of the GO nanosheet appear flat and smooth (Fig. 4C and D). However, at the start of the RPA reaction, the RecA recombinase initially aggregated with the primers, forming nucleoprotein filaments, which were absorbed by the GO nanosheet and other RPA reagents, including metal ions,

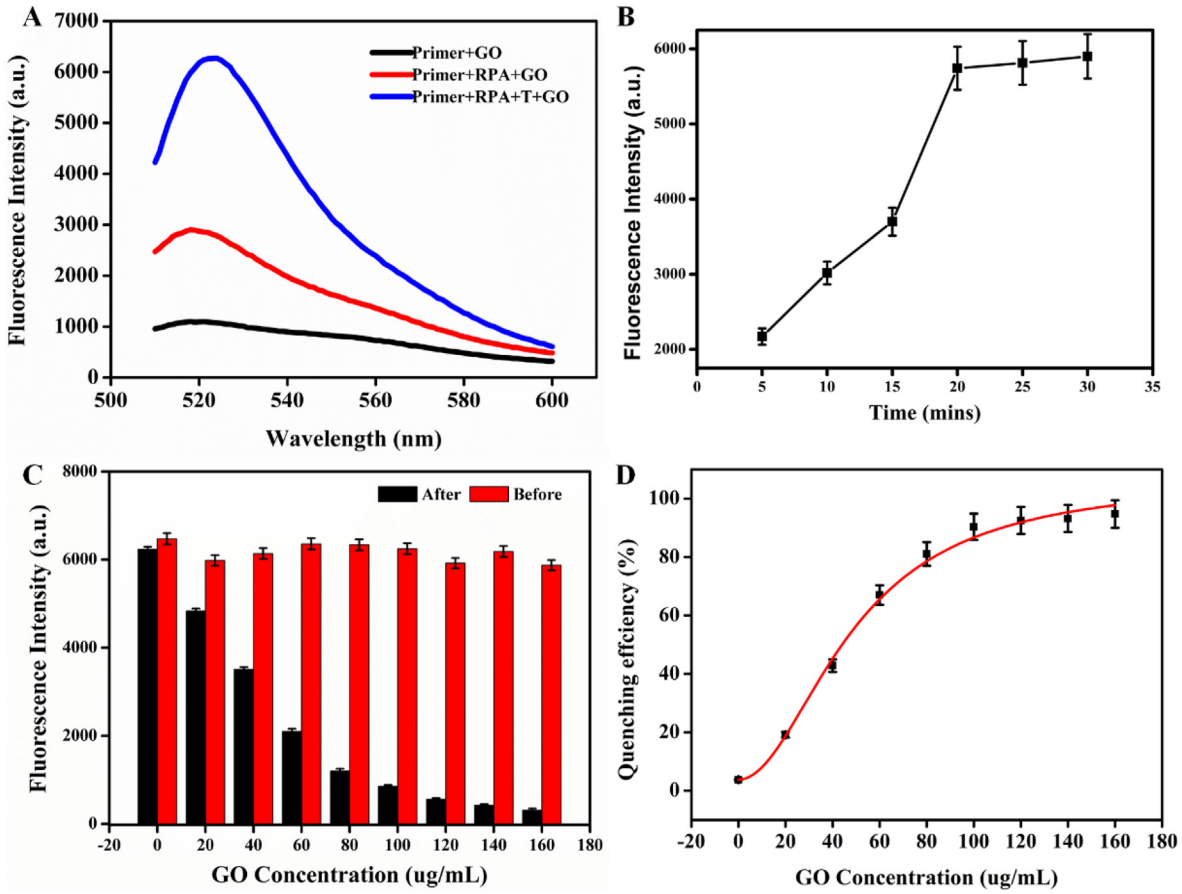

Fig. 5. The performance of GORB in the optimized conditions. A, The fluorescence emission spectra of three types of sensing systems, namely the RPA-amplified sensing system (Primer + RPA + T + GO), the traditional GO-aided system without RPA amplification (Primer + GO), and a system revealing the background signal without target DNA (Primer + RPA + GO). B, Optimization of GM incubation time. GO, and the probes were incubated with transgenic soybeans via the RPA reaction for 5–30 min C. The fluorescence intensity at various GO concentrations ranging from 0 μg/mL to 160 μg/mL. D, The quenching efficiency of the GO nanosheets. All the reactions were measured 10 min after the addition of GO.

polymerases, and primers. Then, the GO nanosheet surface changed to appear rough and fluffy (Fig. 4E and F). The tentacle-shaped nucleoprotein filaments covered the surface of the GO nanosheet, scanning the template DNA for homologous sequences and catalyzing strand exchange at the cognate sites. Moreover, to further analyze the GO absorption, energy dispersive spectroscopy was used to measure the element distribution over the surface of the GO nanosheet after the RPA reaction. The analysis of the tentacle-covered GO nanosheets is shown in Fig. 4A. The main element C (red), O (green) came from GO, proteins and nucleotide acids. The Na, Pt, P, K, Cl, and Mg elements were derived from the reaction buffer and were present on the surface of the GO nanosheet.

3.5. Feasibility of GROB

The reaction was investigated by comparing the fluorescence of various systems to verify the feasibility of the method. Fig. 5A shows the fluorescence emission spectra of the RPA-amplified sensing system (Primer + RPA + T + GO), the traditional GO-aided system without RPA amplification (Primer + GO), and a system revealing the background signal without target DNA (Primer + RPA + GO). The fluorescence of the labeled FAM at the 5′ ends of the forward primer was low due to fluorescence quenching by the GO nanosheets without RPA amplification. Moreover, the fluorescence signal was enhanced by the RPA reaction without a target, but the signal was lower. After introducing the target DNA and RPA reaction, the fluorescence signal increased significantly, almost six-fold. A substantial change was observed in the response signal, demonstrating the feasibility of the biosensor system.

3.6. Optimization of GORB

The GO nanosheet concentration and GM incubation time were optimized to achieve the best performance of the designed biosensor. The GO nanosheets were used as a fluorescence quencher, the quenching ability of which was tested by measuring the fluorescence signal at various GO concentrations ranging from 0 μg/mL to 160 μg/mL, as illustrated in Fig. 5. The FAM-labeled forward primer under contained a concentration of 1.5 μL (10 μM). The fluorescence signal decreased significantly in conjunction with an increase in the GO concentration (Fig. 5A). The quenching efficiency of GO was defined as $QE = (F_0\text{-}F)/F_0$, where F_0 and F represent the fluorescence intensities before and after the addition of GO. The quenching efficiency reached 90% when the GO concentration exceeded 120 μg/mL, which was selected as the optimal concentration for all the experiments.

In addition, the GM reaction incubation time was essential in influencing the RPA signal amplification process. Therefore, this study investigated the effect of different incubation times ranging from 5 min to 30 min on the fluorescence intensity of RPA products (Fig. 5B). The results showed that the fluorescence intensities became higher as the time increased from 5 min to 30 min, after

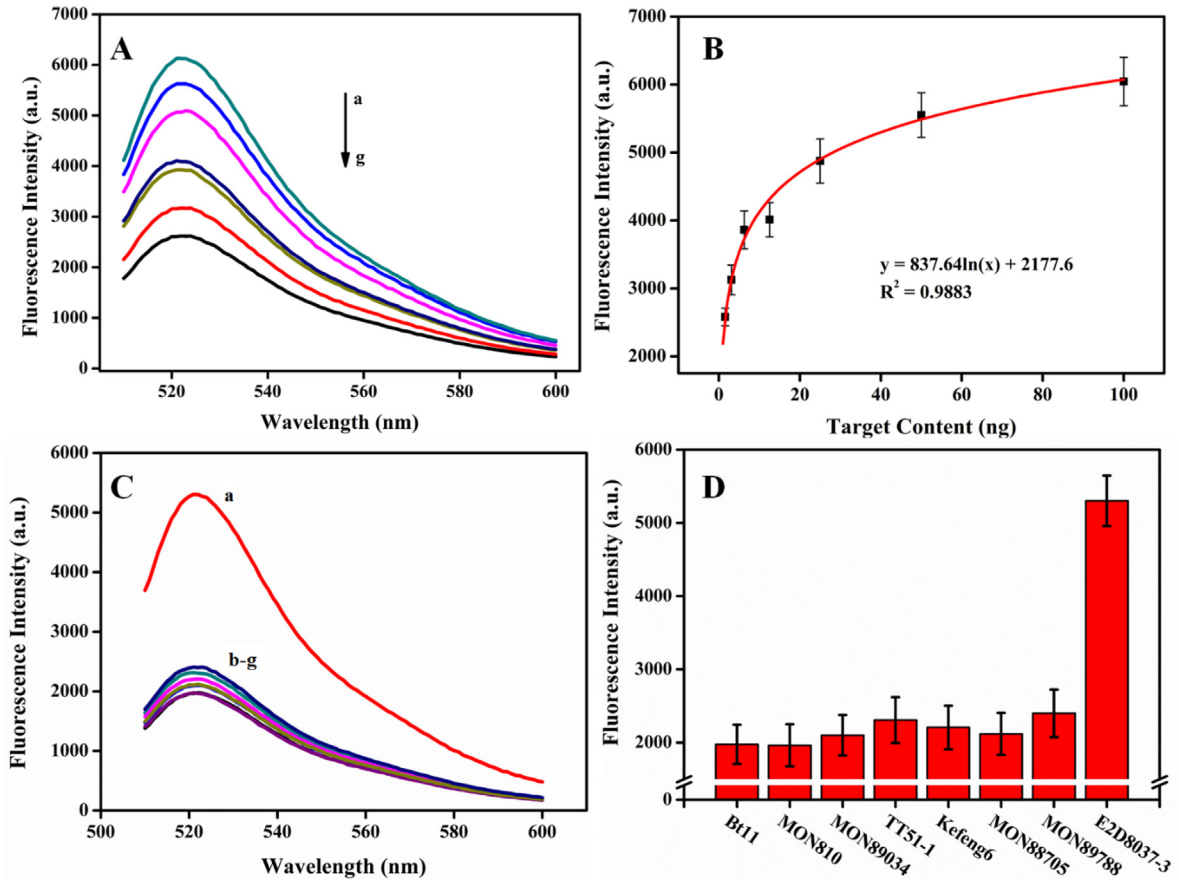

Fig. 6. Sensitivity and selectivity analysis of GORB. A, the fluorescence spectra of the fluorescence intensity of the RPA products in the presence of different nucleic acid concentrations ranging from 0 to 100 ng: a, 100 ng; b, 50 ng; c, 25 ng; d, 12.5 ng; e, 6.25 ng; f, 3.125 ng; g, 1.5625 ng. B, The linear relationship between the fluorescence intensity and nucleic acid concentration. The error bars represent the standard deviations of three repeated experiments. C, the fluorescence spectra of the fluorescence intensity of RPA products in the presence of various materials: GM maize Bt11, MON810 and MON89034, GM rice TT51-1 and Kefeng6, GM soybean MON89788, MON87705, and E2D8037-3. D, the bars represent the fluorescence intensity of the assay in the presence of various materials. The error bars represent the standard deviations of three repeated experiments.

Table 3
Analytical performances of different biosensors.

Technique	Combination	Linear range	Sensitivity	Time	Target	Ref
Electrochemistry	EBFC	0.02–5 ng/mL	7.90 pg/mL	~2 h	thrombin	[34]
EBFC	Cruciform DNA	0.5 fM-10 pM	0.15 fM	<1.5 h	miRNA	[35]
Electrochemistry	CHA	100 aM-100 pM	10 aM	<2 h	miRNA	[36]
Electrochemistry	HCR	100 fM-10 nM	11.6 fM	<1.5 h	thrombin	[37]
Fluorescence	Signal amplification	10 pM-2 nM	4.2 pM	~1day	miRNA	[38]
Fluorescence	HCR	10 pM-10 nM	10 pM	2 h	miRNA	[39]
Electrochemistry	ATRP	1 aM-100 fM	0.213 aM	~2.5 h	DNA	[40]
Electrochemistry	Nanoflower	1100-1.21 × 10^5 copies/mL	1100 copies/mL	~1.5 h	DNA	[41]
Fluorescence	RPA	1.5–100 ng	1.5 ng	30 min	DNA	This work

EBFC: enzymatic biofuel cell; CHA: catalytic hairpin assembly; HCR: hybridization chain reaction; ATRP: atom transfer radical polymerization; RPA: recombinase polymerase amplification.

which the fluorescence signal reached a plateau. Consequently, 30 min was selected as the optimal GM incubation time. These findings further illustrated that the designed probes exhibited high sensitivity, selectivity, and reaction efficiency for GM detection.

3.7. Sensitivity and selectivity analysis

The sensitivity analysis of the biosensor was performed in optimal experimental conditions, while the sensitivity was determined by changing the concentration of the target DNA. As shown in Fig. 6A, GORB was incubated with RNAi transgenic soybeans. The fluorescence intensity became higher in conjunction with an increase in the target DNA concentration, while a positive correlation was evident between the target DNA and the fluorescence intensity. The detection range was 1.5–100 ng, and the lowest LOD was 1.5 ng, exhibiting an excellent relationship. Comparing with reported methods listed in Table 3, these results indicated that the proposed GORB was highly sensitive for GM detection, achieving on-site detection.

GM maize Bt11, MON810 and MON89034, GM rice TT51-1 and Kefeng6, GM soybean MON89788, MON87705, and E2D8037-3 were selected to investigate the selectivity of the biosensor. The interfering materials were incubated with GO via the RPA reaction, and their fluorescence intensities were measured. Fig. 6C shows

that the highest fluorescence intensity peak was produced by E2D8037-3 compared with other biological interfering materials, exhibiting the highest fluorescence response. Therefore, GORB displayed high selectivity for E2D8037-3 in the presence of interfering materials.

4. Conclusions

This study verifies the fact that GO nanosheets can improve the amplification efficiency of the RPA reaction. Though fluorescence and SEM analysis, GO nanosheets could absorb the reagents of reaction and trigger the aggregation effect in local, which promote the amplification efficiency of RPA. Therefore, this study investigates a “turn-on” biosensor based on GO and RPA for the selective and sensitive detection of RNAi transgenic plants. This method has a LOD of 1.5 ng genome DNA. The joint action of GO and RPA further amplifies the detection signal and improve the sensitivity of the biosensor. GORB is inexpensive and highly sensitive with a lower fluorescence background compared to other traditional detection methods. Moreover, this proposed biosensor can be applied for GM-specific assays and exhibit significant potential for related biochemical research and clinical analysis.

CRediT authorship contribution statement

Kai Li: Conceptualization, Methodology, Validation, Formal analysis, Data curation, Writing – original draft. **Zhan Lei:** Methodology, Validation, Formal analysis, Writing – review & editing, Validation. **Chen Zhang:** Investigation, Data curation, Resources. **Longjiao Zhu:** Formal analysis, Validation, Investigation. **Kunlun Huang:** Conceptualization, Methodology, Supervision. **Ying Shang:** Conceptualization, Project administration, Formal analysis. **Wentao Xu:** Conceptualization, Supervision, Project administration, Funding acquisition.

Declaration of competing interest

The authors declare that they have no known competing financial interests or personal relationships that could have appeared to influence the work reported in this paper.

Acknowledgment

The authors deeply appreciate the Hebei Province key research and development program (21372801D), and the 2115 Talent Development Program of China Agricultural University (00109016) for financial support to this work.

Appendix A. Supplementary data

Supplementary data to this article can be found online at https://doi.org/10.1016/j.aca.2021.339222.

References

[1] L. Huang, J. Chen, L. Gan, J. Wang, S. Dong, Single-atom nanozymes, Sci. Adv. 5 (5) (2019).
[2] Q. Hu, H. Li, L. Wang, H. Gu, C. Fan, DNA nanotechnology-enabled drug delivery systems, Chem. Rev. 119 (10) (2019) 6459–6506.
[3] M.S. Desai, S.W. Lee, Protein-based functional nanomaterial design for bioengineering applications, NanoBiotechnology 7 (1) (2015) 69–97.
[4] R. Mohammadinejad, M.A. Moosavi, S. Tavakol, D.Ö. Vardar, A. Hosseini, M. Rahmati, L. Dini, S. Hussain, A. Mandegary, D.J. Klionsky, Necrotic, apoptotic and autophagic cell fates triggered by nanoparticles, Autophagy 15 (1) (2019) 4–33.
[5] J.R. Lead, G.E. Batley, P.J.J. Alvarez, M.-N. Croteau, R.D. Handy, M.J. McLaughlin, J.D. Judy, K. Schirmer, Nanomaterials in the environment: behavior, fate, bioavailability, and effects—an updated review, Environ. Toxicol. Chem. 37 (8) (2018) 2029–2063.
[6] Z. Peng, X. Liu, W. Zhang, Z. Zeng, Z. Liu, C. Zhang, Y. Liu, B. Shao, Q. Liang, W. Tang, X. Yuan, Advances in the application, toxicity and degradation of carbon nanomaterials in environment: a review, Environ. Int. 134 (2020).
[7] W. Wan, J.T.W. Yeow, The effects of gold nanoparticles with different sizes on polymerase chain reaction efficiency, Nanotechnology 20 (32) (2009), 325702.
[8] W. Yang, L. Mi, X. Cao, X. Zhang, C. Fan, J.J.N. Hu, Evaluation of gold nanoparticles as the additive in real-time polymerase chain reaction with, SYBR Green I dye 19 (25) (2008), 255101.
[9] H. Li, J. Huang, J. Lu, H. An, X. Zhang, Z. Zhang, C. Fan, J. Hu, Nanoparticle PCR: Nanogold-Assisted PCR with Enhanced Specificity, 2005.
[10] D. Cui, F. Tian, Y. Kong, I. Titushikin, H. Gao, Effects of single-walled carbon nanotubes on the polymerase chain reaction, Nanotechnology 15 (1) (2014) 154–157.
[11] J.Y. Park, S.H. Back, S.J. Chang, S.J. Lee, K.G. Lee, T.J. Park, Dopamine-assisted synthesis of carbon-coated silica for PCR enhancement, ACS Appl. Mater. Interfaces 7 (28) (2015) 15633–15640.
[12] H. Wang, L. Wang, L. Yuan, W. Yang, J.L. Brash, H. Chen, Inhibitory effect of silicon nanowires on the polymerase chain reaction, Nanotechnology 23 (36) (2012), 365101.
[13] K.R. Abdul, P.J. Sonawane, B.K. Sasi, B.S. Sahu, T. Pradeep, S.K. Das, N.R. Mahapatra, Enhancement in the efficiency of polymerase chain reaction by TiO_2 nanoparticles: crucial role of enhanced thermal conductivity, Nanotechnology 21 (25) (2010), 255704.
[14] Z. Zhang, M. Wang, H. An, An aqueous suspension of carbon nanopowder enhances the efficiency of polymerase chain reaction, Nanotechnology 18 (35) (2007), 355706.
[15] R. Khaliq, R. Kafafy Abdul, H.M. Salleh, W.F. Faris, Enhancing the efficiency of polymerase chain reaction using graphene nanoflakes, Nanotechnology 23 (45) (2012), 455106.
[16] L. Zhang, X. Jing, W. Chen, J. Bai, L. Vasseur, W. He, M. You, Selection of reference genes for expression analysis of plant-derived microRNAs in Plutella xylostella using qRT-PCR and ddPCR, PLoS One 14 (8) (2019).
[17] M.-J. Kim, H.-Y. Kim, A fast multiplex real-time PCR assay for simultaneous detection of pork, chicken, and beef in commercial processed meat products, LWT Food Sci. Technol. 114 (2019).
[18] A.C. Vinayaka, T.A. Ngo, K. Kant, P. Engelsmann, V.P. Dave, M.-A. Shahbazi, A. Wolff, D.D. Bang, Rapid detection of Salmonella enterica in food samples by a novel approach with combination of sample concentration and direct PCR, Biosens. Bioelectron. 129 (2019) 224–230.
[19] Y.W. Tang, J.E. Schmitz, D.H. Persing, C.W. Stratton, Laboratory diagnosis of COVID-19: current issues and challenges, J. Clin. Microbiol. 58 (6) (2020).
[20] Y. Zhao, X. Zuo, Q. Li, F. Chen, Y.-R. Chen, J. Deng, D. Han, C. Hao, F. Huang, Y. Huang, G. Ke, H. Kuang, F. Li, J. Li, M. Li, N. Li, Z. Lin, D. Liu, J. Liu, L. Liu, X. Liu, C. Lu, F. Luo, X. Mao, J. Sun, B. Tang, F. Wang, J. Wang, L. Wang, S. Wang, L. Wu, Z.-S. Wu, F. Xia, C. Xu, Y. Yang, B.-F. Yuan, Q. Yuan, C. Zhang, Z. Zhu, C. Yang, X.-B. Zhang, H. Yang, W. Tan, C. Fan, Nucleic Acids Analysis, Science China Chemistry, 2020.
[21] Y. Zhu, S. Murali, W. Cai, X. Li, J.W. Suk, J.R. Potts, R.S. Ruoff, Graphene and graphene oxide: synthesis, properties, and applications, Adv. Mater. 22 (35) (2010) 3906–3924.
[22] Z. Zang, X. Zeng, M. Wang, W. Hu, C. Liu, X. Tang, Tunable photoluminescence of water-soluble AgInZnS–graphene oxide (GO) nanocomposites and their application in-vivo bioimaging, Sensor. Actuator. B Chem. (2017), S092540051731359X.
[23] S. Chu, W. Huang, F. Shen, T. Li, S. Li, W. Xu, C. Lv, Q. Luo, J. Liu, Graphene oxide-based colorimetric detection of organophosphorus pesticides via a multi-enzyme cascade reaction, Nanoscale 12 (10) (2020) 5829–5833.
[24] P.K. Smitha, C. Bathula, K.N. Chandrashekara, M. Das, Usage of graphene oxide in fluorescence quenching-linked immunosorbent assay for the detection of Cry2Ab protein present in transgenic plants, J. Agric. Food Chem. 68 (11) (2020) 3656–3662.
[25] N.A. Samak, M.S. Selim, Z. Hao, J. Xing, Controlled-synthesis of alumina-graphene oxide nanocomposite coupled with DNA/sulfide fluorophore for eco-friendly "Turn off/on" H2S nanobiosensor, Talanta 211 (2020).
[26] M. Li, X. Zhou, S. Guo, N. Wu, Detection of lead (II) with a "turn-on" fluorescent biosensor based on energy transfer from CdSe/ZnS quantum dots to graphene oxide, Biosens. Bioelectron. 43 (2013) 69–74.
[27] M. Liu, H. Zhao, S. Chen, H. Yu, Y. Zhang, X. Quan, A "turn-on" fluorescent copper biosensor based on DNA cleavage-dependent graphene-quenched DNAzyme, Biosens. Bioelectron. 26 (10) (2011) 4111–4116.
[28] J. Huang, X. Gao, J. Jia, J.-K. Kim, Z. Li, Graphene oxide-based amplified fluorescent biosensor for Hg2+ detection through hybridization chain reactions, Anal. Chem. 86 (6) (2014) 3209–3215.
[29] S.-Y. Wang, C.-F. Wang, Y.-K. Lv, S.-G. Shen, Fabrication of fluorescent biosensing platform based on graphene oxide-DNA and their application in biomolecule detection, Trac. Trends Anal. Chem. 106 (2018) 53–61.
[30] E. Morales-Narváez, B. Pérez-López, L.B. Pires, A. Merkoçi, Simple Förster Resonance Energy Transfer Evidence for the Ultrahigh Quantum Dot Quenching Efficiency by Graphene Oxide Compared to Other Carbon Structures, Carbon, 2012.
[31] X. Cui, L. Zhu, J. Wu, Y. Hou, P. Wang, Z. Wang, M. Yang, A fluorescent biosensor based on carbon dots-labeled oligodeoxyribonucleotide and graphene oxide for mercury (II) detection, Biosens. Bioelectron. 63 (2015) 506–512.

[32] J.-S. Lee, J. Kim, H. Shin, D.-H. Min, Graphene oxide-based molecular diagnostic biosensor for simultaneous detection of Zika and dengue viruses, 2D Mater. 7 (4) (2020).
[33] J. Jeon, J. Lee, J.-i. So, J. Lee, H. Lee, Y. Chang, S. Shin, J. Jo, C. Ban, Homogeneous fluorescent aptasensor for active tuberculosis diagnosis by direct quantification of circulating TB7.7 based on aptamer beacon with graphene oxide, Sensor. Actuator. B Chem. 317 (2020).
[34] Y. Wang, F. Wang, Z. Han, K. Huang, X. Wang, Z. Liu, S. Wang, Y. Lu, Construction of sandwiched self-powered biosensor based on smart nanostructure and capacitor: toward multiple signal amplification for thrombin detection, Sensor. Actuator. B Chem. 304 (2020), 127418.
[35] F.-T. Wang, Y.-H. Wang, J. Xu, K.-J. Huang, Z.-h. Liu, Y.-f. Lu, S.-y. Wang, Z.-w. Han, Boosting performance of self-powered biosensing device with high-energy enzyme biofuel cells and cruciform DNA, Nano Energy 68 (2020), 104310.
[36] Y.-X. Chen, X. Wu, K.-J. Huang, A sandwich-type electrochemical biosensing platform for microRNA-21 detection using carbon sphere-MoS2 and catalyzed hairpin assembly for signal amplification, Sensor. Actuator. B Chem. 270 (2018) 179–186.
[37] Y.-X. Chen, K.-J. Huang, L.-L. He, Y.-H. Wang, Tetrahedral DNA probe coupling with hybridization chain reaction for competitive thrombin aptasensor, Biosens. Bioelectron. 100 (2018) 274–281.
[38] Y. Xia, L. Wang, J. Li, X. Chen, J. Lan, A. Yan, Y. Lei, S. Yang, H. Yang, J. Chen, A ratiometric fluorescent bioprobe based on carbon dots and acridone derivate for signal amplification detection exosomal microRNA, Anal. Chem. 90 (15) (2018) 8969–8976.
[39] D. He, L. Hai, H. Wang, R. Wu, H.-W. Li, Enzyme-free quantification of exosomal microRNA by the target-triggered assembly of the polymer DNAzyme nanostructure, Analyst 143 (4) (2018) 813–816.
[40] Q. Liu, J. Liu, H. Yang, X. Wang, J. Kong, X. Zhang, Highly sensitive lung cancer DNA detection via GO enhancing eATRP signal amplification, Microchem. J. 160 (2021), 105766.
[41] F. Zhao, Y. Bai, L. Cao, G. Han, C. Fang, S. Wei, Z. Chen, New electrochemical DNA sensor based on nanoflowers of Cu3(PO4)2-BSA-GO for hepatitis B virus DNA detection, J. Electroanal. Chem. 867 (2020), 114184.